

## Article

# Active Power Assist with Equivalent Force on Connection for Lower Limb Exoskeleton Robots

Jing Deng <sup>1,2</sup>, Wenzheng Jiang <sup>2</sup>, Haibo Gao <sup>1</sup>, Mantian Li <sup>3</sup> and Yapeng Shi <sup>1,4,5,\*</sup>

- <sup>1</sup> State Key Laboratory of Robotics and System, Harbin Institute of Technology, Harbin 150001, China; 13b308005@hit.edu.cn (J.D.); gaohaibo@hit.edu.cn (H.G.)
- <sup>2</sup> Shenzhen Academy of Aerospace Technology, Shenzhen 518063, China; airrc@protonmail.com
- <sup>3</sup> Institute of Intelligent Manufacturing Technology, Shenzhen Polytechnic University, Shenzhen 518055, China; limt@hit.edu.cn
- <sup>4</sup> Faculty of Computing, Harbin Institute of Technology, Harbin 150001, China
- <sup>5</sup> School of Mechanical Engineering, Yanshan University, Qinhuangdao 066004, China
- \* Correspondence: shi.yapeng@hit.edu.cn

**Abstract:** Active power-assist lower limb exoskeleton robots aim to enhance wearer assistance while ensuring wearer comfort and simplifying the exoskeleton's design and control. This study proposes an active assistance method known as Equivalent Force on Connection (EFOC). The EFOC method effectively addresses the limitations encountered in conventional Joint Torque Proportional Compensation (JTPC) approaches. These limitations include the necessity for exoskeleton robot configurations to align with human limb structures for parallel assistance at each lower limb joint, as well as the exoskeleton's inability to contribute a greater proportion of assistance due to the excessive load on specific skeletal and muscular structures, resulting in wearer discomfort. Furthermore, the effectiveness of the EFOC method is evaluated and validated for assistance during both the stance and swing phases of single-leg movements. Finally, the proposed EFOC method is implemented on a hydraulic-driven lower limb exoskeleton robot to assist wearers in squatting, stepping, and jumping locomotion. The experimental results demonstrate that the proposed EFOC method can effectively achieve the desired assistance effect.



**Citation:** Deng, J.; Jiang, W.; Gao, H.; Li, M.; Shi, Y. Active Power Assist with Equivalent Force on Connection for Lower Limb Exoskeleton Robots. *Actuators* **2024**, *13*, 212. <https://doi.org/10.3390/act13060212>

Academic Editors: Jorge L. Candiotti, Jonathan Duvall, Brad Duerstock and Jongbae Kim

Received: 1 May 2024

Revised: 20 May 2024

Accepted: 1 June 2024

Published: 5 June 2024



**Copyright:** © 2024 by the authors. Licensee MDPI, Basel, Switzerland. This article is an open access article distributed under the terms and conditions of the Creative Commons Attribution (CC BY) license (<https://creativecommons.org/licenses/by/4.0/>).

**Keywords:** equivalent force on connection; joint torque proportional compensation; lower limb exoskeleton robots

## 1. Introduction

The lower limb exoskeleton robot is a type of wearable robotic device intended to assist the wearer's lower limbs [1,2]. This has motivated numerous researchers to undertake the design and development of lower limb exoskeleton robots for various promising applications, including rescue services, heavy load carrying, healthcare, and rehabilitation, among others [3,4]. As a human-machine coupled system within a human-in-the-loop paradigm, a central characteristic of lower limb exoskeleton robots is their ability to synchronize movements and coordinate with the wearer's legs [5].

Control methods for active power-assist lower limb exoskeleton robots vary depending on their specific applications. Lower limb exoskeleton robots designed for rehabilitation purposes often employ pre-programmed motion control methods [6]. For instance, platforms, such as Lokomat [7], ReWalk [8], Ekso [9], and AiWalker [10], utilize pre-recorded normal gait data to facilitate passive rehabilitation for patients. These systems aim to prevent joint contractures, venous thrombosis, and muscle atrophy in affected limbs while also utilizing visual feedback stimulation from virtual environments to aid in neural pathway reconstruction and gait retraining [11]. However, this approach relies on the exoskeleton robots completely replacing the wearer's control over lower limb movement, thus preventing the wearer's involvement in lower limb control. As a result, this method is typically

restricted to use with treadmill frames or with the assistance of crutches for support and control [6].

In the scenarios of enhancing walking endurance and carrying heavy loads, the movement of the lower limbs exhibits repetition. This repeatability significantly benefits the control design of lower limb exoskeleton robots. The theory of gait recognition and stage recognition categorizes human gait into various types, such as walking, running, stair climbing, etc., and further subdivides the gait cycle into stages including swing and stance phases [12,13]. Based on the gait sample profiles and parameters such as stride duration and stride length, the limb motions of exoskeleton robots are synthesized, enabling coordinated movement with the human [14]. Scholars have attempted to identify gait patterns using various measurement methods. Novel methods are continually proposed and validated, with the overarching aim of improving the accuracy and speed of gait recognition [13].

To improve the cooperation between exoskeleton robots and the wearer, on the one hand, the wearer dominates the lower limb movement. This maintains the wearer's balance control, cooperated movements, and rapid response capabilities in complex environments [15]. Exoskeleton robots are designed to follow the wearer's movements, conform perfectly to the wearer's movements, and bear external loads instead of the wearer [16]. On the other hand, the motion intention of the wearer is sensed through various measurement methods to control the exoskeleton robot, such as measuring the interaction force or position tracking error between the wearer and the exoskeleton robot [17,18]; through the sensitivity amplification control (SAM) method [19]; detecting the wearer's biological signals, including surface electromyography (sEMG) signals [20] and the brain-machine interface [21].

Regardless of the control method employed, the motion control module and the joint actuation module of exoskeleton robots function as a cascaded closed-loop control system, with the joint actuation module serving as the inner loop and the motion control module as the outer loop [22–24]. The motion control module is tasked with calculating appropriate motion trajectories for the exoskeleton limbs, providing a specified level of assistance and ensuring that the movement of the exoskeleton is coordinated with the wearer's limbs [25].

For lower limb exoskeleton robots, the pitch joints of the hip, knee, and ankle of each leg provide support for the wearer. Upon estimating the desired torques at each joint, these desired torques are proportionally mapped to the corresponding exoskeleton joints to apply active torques, termed as Joint Torque Proportional Compensation (JTPC), based on the active power-assist coefficients. This method provides a linear relationship between the assisted torques to each joint and the desired torques required by the joints to conform to match the human body movement. To achieve accurate Joint Torque Proportional Compensation, the designed exoskeleton robot mechanism has to closely resemble the configuration of the human lower limb, with the wearer's trunk, thigh, and calf secured to the corresponding links of the exoskeleton robots. Flexible materials are employed within the exoskeleton robot to ensure both strap position securing and wearer comfort during motion. In contrast to the JTPC method, this work proposes an Equivalent Force on Connection (EFOC) method that leverages the human-machine coupling characteristics. The motion control module focuses solely on the interaction information between the exoskeleton and the wearer's trunk and foot connection points, without the need to consider the force and position tracking of each joint.

The innovative contributions of this work can be summarized as follows:

- The assistance actuators of the exoskeleton do not need to be parallel to each joint of the human lower limb, improving the flexibility of structural design.
- The number of human-machine connection points is significantly reduced, allowing for the relocation of connection points to positions on the human body capable of withstanding higher loads.
- Instead of accurately measuring the torque at each joint, a feedback controller can be utilized by simply measuring the interface forces between the wearer and the exoskeleton robot at the torso and foot-end attachment points.

- There is no need for sensors on the wearer, such as sEMG, to improve wearer comfort.
- It contributes to improving the loading conditions on the wearer's skeletal system, reducing the stress on the bones.

The remainder of this paper is organized as follows: Section 2 provides an in-depth exploration of the MTPC assistance method and analyzes its limitations. Following this, Section 3 delves into the detailed implementation processes of the EFOC method. The EFOC method is shown to achieve comparable assistance effects to the MTPC method while overcoming its limitations. Squatting, walking, and jumping motions were tested on a hydraulically actuated exoskeleton robot, and the results of the experiments are discussed in Section 4. Section 5 provides a comprehensive summary of this work and outlines potential directions for future work.

## 2. MTPC Power-Assist Method

For the convenience of theoretical analysis, it is assumed that the assistance provided by the exoskeleton does not alter the trajectory of human motion, meaning that the total joint torques required for human movement remain constant. In this scenario, with the involvement of the exoskeleton, both the human body and the exoskeleton collaboratively propel the wearer's limb movements. Consequently, the actual joint torques produced by the human body, along with the assisted torques from the exoskeleton, jointly contribute to maintaining the torque required for human movement, as follows:

$$\hat{\tau} = \tau_E + \tau_H, \quad (1)$$

where  $\hat{\tau}$  denotes the total torque required for specified joint movement.  $\tau_E$  and  $\tau_H$  indicate the torques provided by the exoskeleton robot and the human, separately.

We assume that the total joint torque required for joint movement is 100 Nm, and further assume the following:

$$\tau_E = \alpha \hat{\tau}, \quad \alpha \in [-1, 2], \quad (2)$$

where  $\alpha$  denotes the active assistance coefficient of the exoskeleton robot.

As the assistance coefficient varies from  $-1$  to  $2$ , the torques provided by the exoskeleton  $\tau_E$  and those exerted by the human body are illustrated in Figure 1. It is evident that when the signs of  $\tau_E$  and  $\hat{\tau}$  are opposite,  $\alpha < 0$ , indicating a situation where the exoskeleton robot hinders joint movement, so the human body needs to exert a stronger torque to maintain the desired joint trajectory. Conversely, when  $\tau_E$  and  $\hat{\tau}$  have the same sign and  $0 < \alpha \leq 1$ , the joint torque  $\tau_H$  exerted by the human body decreases with the enhancement in  $\tau_E$ , signifying the assisting effect of the exoskeleton. The ideal scenario occurs when  $\tau_E = \hat{\tau}$ , which means the exoskeleton robot seamlessly provides the total joint torque required for human movement, effectively replacing the wearer's muscular effort. Subsequently, if  $\tau_E$  continues to increase beyond  $\hat{\tau}$ , i.e.,  $\alpha > 1$ , overcompensation occurs, and the wearer needs to apply a counteracting torque to maintain the desired joint movement.

Muscle Torque Proportional Compensation (MTPC) is a simple and straightforward method that provides active assistance to each individual joint. This method assumes the exoskeleton robot's capability to calculate the joint torques of the human body in real time and apply a seamlessly equivalent effect to each joint of the human body. Under this assumption, the wearer would theoretically exert minimal effort to execute various movements, which serves as the foundational principle for implementing active assistance in this work. MTPC is, thus, defined as the method by which the exoskeleton robot compensates for a proportion of the joint torques required for maintaining posture and executing movements at each actuated joint.

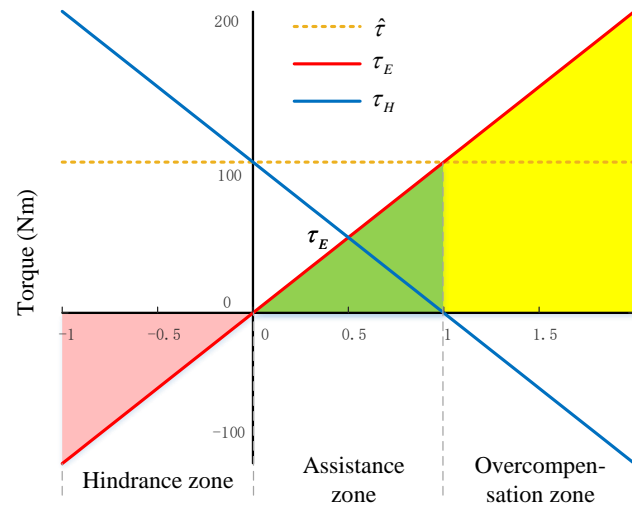


**Figure 1.** Characteristics of the joint torque provided by the exoskeleton robot and the joint torque provided by the wearer vary with the assistance coefficient while maintaining a constant joint torque.

Based on its description, the exoskeleton robot compensates for the total joint torques  $\hat{\tau}$  required for human movement by outputting a certain proportion of joint torque  $\tau_E$ . This assistance is effective as long as the wearer does not need to exert torques exceeding the total joint torques or counteracting torques. It can be expressed as follows:

$$\begin{cases} \hat{\tau} = \tau_H + \tau_E \\ \tau_E = \alpha \hat{\tau}, (0 \leq \alpha \leq 1) \end{cases} \quad (3)$$

Assuming that the exoskeleton robot assists the human in performing the same movement, the total power of the joint remains unchanged. From an energetic perspective, when a human performs a certain movement, the power required by the joint is:

$$P = \hat{\tau}\omega = P_H + P_E = \tau_H\omega + \tau_E\omega \quad (4)$$

where  $P_H$  represents the power exerted by the human, and  $P_E$  denotes the power provided by the exoskeleton.  $\omega$  denotes the angular velocity of the corresponding joint. Combining Equations (3) and (4), we can derive:

$$\begin{cases} |\tau_H| = |1 - \alpha| \cdot |\hat{\tau}| \leq |\hat{\tau}| \\ P_H = (1 - \alpha) \cdot P \leq P \end{cases} \quad (5)$$

The conditions for achieving active assistance can be deduced from the above analysis: the auxiliary joint torque exerted by the exoskeleton on the human must align with the required joint torque of the human, and the magnitude of the assistance should be less than the required joint torque of the human, i.e., the assistance coefficient  $\alpha \in [0, 1]$ . The larger the assistance coefficient, the stronger the assistance provided by the exoskeleton, and the lesser the wearer’s involvement in motion control. Taking into account errors in motion intention perception, wearer safety, and the dynamic limitations of the exoskeleton robot, this study restricts the assistance coefficient to be within 0.25.

The joint power profiles before and after assistance are illustrated in Figure 2. With exoskeletal assistance, the mechanical power of the human joint decreases proportionally. It can be seen that the MTPC method can reduce both the amplitude of the wearer’s joint torque and joint power, theoretically achieving active assistance. More importantly, this method is applicable to all four quadrants, namely,  $(\hat{\tau}+, \omega+)$ ,  $(\hat{\tau}-, \omega+)$ ,  $(\hat{\tau}-, \omega-)$ , and  $(\hat{\tau}+, \omega-)$ , without distinguishing whether the body link is moving forward, backward, accelerating, or decelerating. It eliminates the need to differentiate between walking, running, jumping, or any other movements. This circumvents a series of complex issues

such as gait recognition and gait cycle segmentation. This is a universal method, and its significance lies in its ability to support arbitrary human movements.

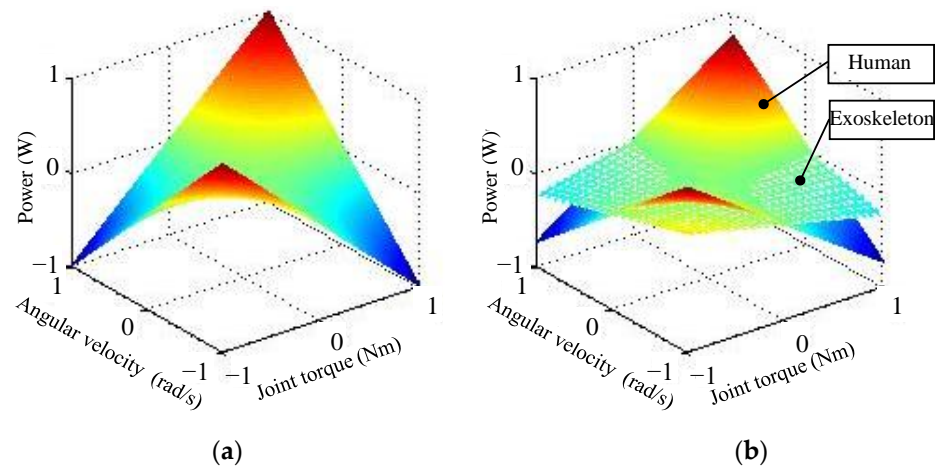


**Figure 2.** Influence of the MTPC active power assist on human joint power. (a) Without assistance; (b) with exoskeleton robot assistance.

To validate the efficacy of the MTPC method on the human body, a dynamics model with dimensions and mass distribution resembling the human body was established. A series of multibody dynamics simulations were conducted for both swing and stance legs. The joint torque profiles before and after the assistance were a comparison while maintaining the same limb trajectories.

A simplified three-link model representing a single leg was established in the sagittal plane. The 3D model was imported into Matlab's Simscape (2022b) for multibody dynamics simulation [26]. The torso was fixed in place, with the torso, thigh, calf, and foot sequentially connected through hip, knee, and ankle joints. The trajectory of the foot end was imported to drive the single leg to perform swing motion, obtaining joint angle curves for the hip, knee, and ankle joints ( $Q_h(t)$ ,  $Q_k(t)$ ,  $Q_a(t)$ ). These joint angle curves were then used to drive the single-leg model, yielding joint torque curves for the hip, knee, and ankle joints ( $T_h(t)$ ,  $T_k(t)$ ,  $T_a(t)$ ). The three rotational joints of the human single-leg model were set to position control mode, each parallelly equipped with a torque-driven assistance joint. The human joint was driven by angle profiles ( $Q_h(t)$ ,  $Q_k(t)$ ,  $Q_a(t)$ ), while the assistance joint was driven by torque profiles ( $\alpha T_h(t)$ ,  $\alpha T_k(t)$ ,  $\alpha T_a(t)$ ), with the assistance coefficient denoted as  $\alpha$ .

Similarly, a single-leg stance phase model was established with the foot end set as fixed. By importing the motion trajectory of the torso and converting it into angular curves for the hip, knee, and ankle joints, the stance leg was driven to perform a squat motion. The remaining steps were similar to the swing phase simulation. In this work,  $\alpha$  was set to 0.2. The simulation model is illustrated in Figure 3.

A comparison of human joint torques before and after assistance is depicted in Figure 4. Without assistance, the peak torques of the hip, knee, and ankle joints during the single-leg swing motion were 55.7 Nm, 23.5 Nm, and 6.4 Nm, respectively. After applying assistance using the MTPC method, the peak torques for hip, knee, and ankle joints decreased to 43.8 Nm, 19.4 Nm, and 5.2 Nm, respectively. During the stance phase, similar phenomena can be observed. The peak joint torques of the hip, knee, and ankle joints before assistance were 70.3 Nm, 280.8 Nm, and 16.9 Nm, respectively. After assistance, the peak joint torques for the hip, knee, and ankle decreased to 56.4 Nm, 226.2 Nm, and 13.6 Nm, respectively.

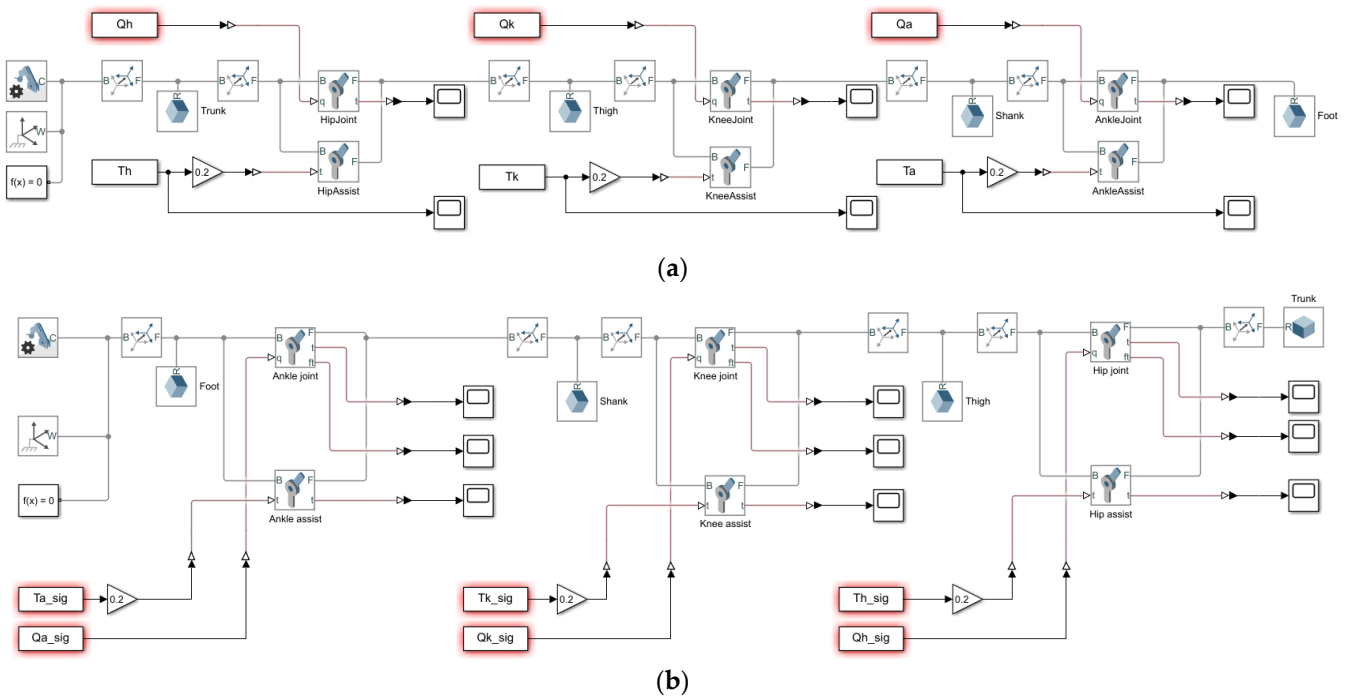


**Figure 3.** Simulation models of MTPC power assists with a single leg in the sagittal plane. (a) The simulation model of the single leg during the swing phase; (b) the simulation model of the single leg during the stance phase.

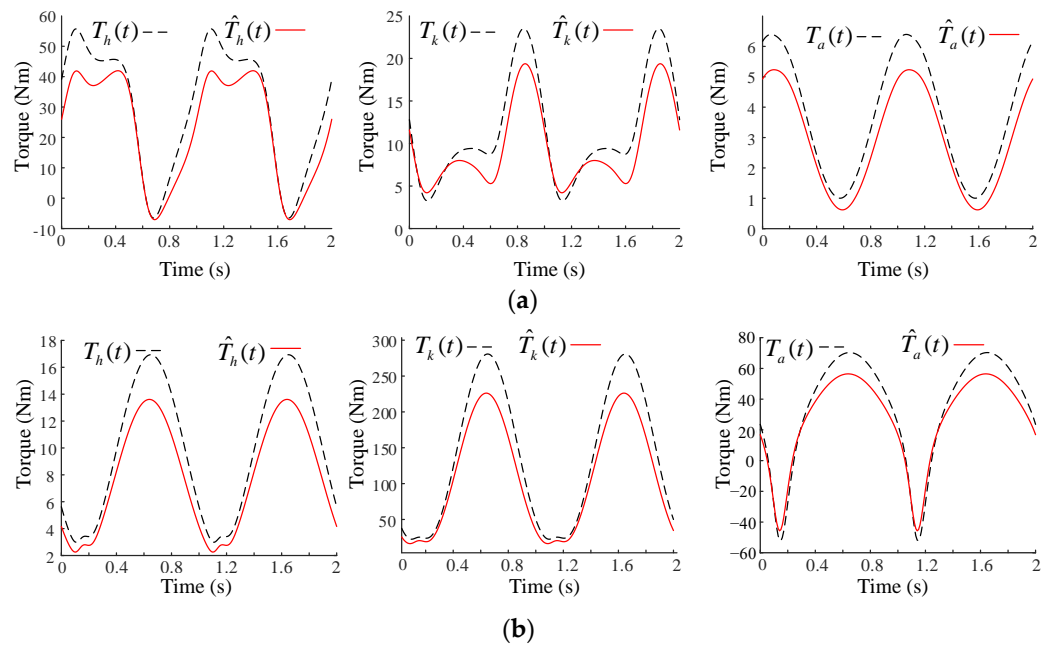


**Figure 4.** Comparison of the joint torque profiles with and without MTPC active assistance. The black dashed curves represent the joint torque profiles without assistance, while the red curves represent the joint torque profiles after assistance. (a) Joint torque profiles with and without assistance during swing motion; (b) joint torque profiles with and without assistance during squatting.

From the simulated results presented above, it is evident that the MTPC method achieves the objective of reducing human joint torques. Simultaneously, the reduction in human joint torques exhibits a relatively stable proportional relationship.

However, the implementation of the MTPC method poses challenges as it requires the parallel connection of the exoskeleton’s actuation components with human joints.



Technically, this poses difficulties for several reasons: Firstly, the loads exerted by the exoskeleton on the human body primarily act on the skin of the body. Apart from areas, such as the plantar surface, hip, and anterior shank, it is difficult for other areas of the human body to bear large external loads for a long time. Secondly, although the actuation method parallel to human joints reduces muscular forces, it may lead to an increase in shear stress on the bones, as illustrated in Figure 5, which is incongruent with the load-bearing characteristics of the human skeletal system. Considering the varying load-bearing capacities of different regions of the human body, establishing the human–machine connection points in areas capable of withstanding significant loads becomes essential. In such cases, the MTPC method may not be applicable, especially in scenarios requiring assistance to multiple joints simultaneously.

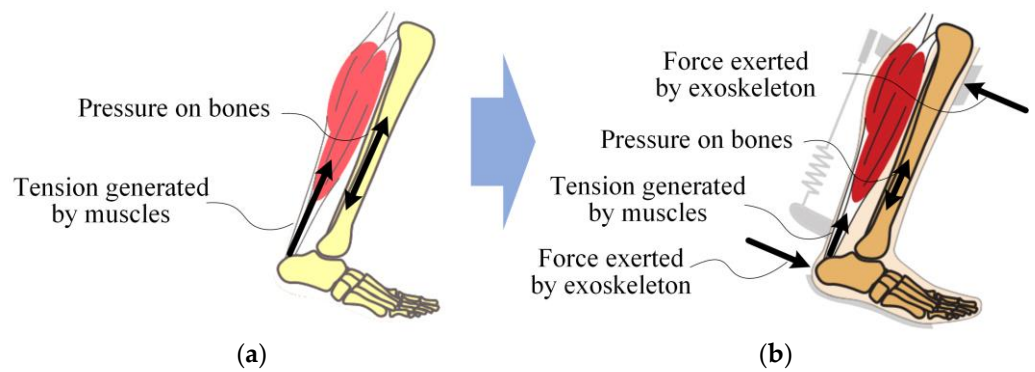


**Figure 5.** Changes in the pressure force on the calf bone before and after the assistance of an exoskeleton robot. (a) Normal force on the calf bone; (b) shear stress on the calf bone.

### 3. EFOC Power-Assist Method

Addressing the limitations of the MTPC method and recognizing the necessity to simultaneously assist multiple joints in this work, we propose an improved approach—the Equivalent Force on Connection (EFOC) method. The underlying concept of this method is to apply equivalent assisting force at the human–machine connection points, thereby proportionally reducing the drive torques at various joints of the human body. From the perspective of minimizing muscular effort, this approach may achieve similar results to MTPC.

The single-leg model with hip, knee, and ankle joints is illustrated in Figure 6. The swing phase of the EFOC method converts the required joint torques ( $\hat{\tau}_{hip}$ ,  $\hat{\tau}_{knee}$ ,  $\hat{\tau}_{ankle}$ ) into equivalent foot-end contact forces ( $\hat{F}_{fx}$ ,  $\hat{F}_{fz}$ ,  $\hat{\tau}_{fy}$ ) for the swing leg or equivalent hip contact forces ( $\hat{F}_{tx}$ ,  $\hat{F}_{tz}$ ,  $\hat{\tau}_{ty}$ ) for the supporting torso, according to the swing or stance phases.

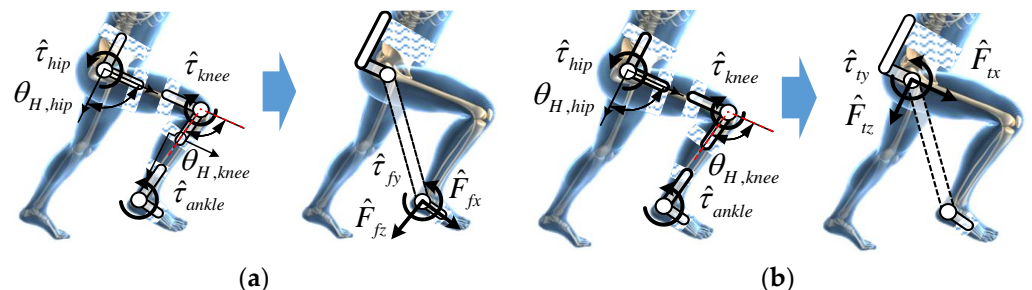


**Figure 6.** Force analysis diagram of active assistance of exoskeleton robots with EFOC method. (a) Assistance force generated for swing leg; (b) assistance force generated for stance leg.

This method treats the human leg as a force transmission mechanism, and the equivalent foot-end contact forces can be resolved based on the force balance equation. With

the assumption of a fixed hip for the swing leg, the coordinates of the knee joint in the hip coordinate system are denoted as:

$$\begin{cases} x_k = l_T \sin(\theta_{H,hip}) \\ z_k = l_T \cos(\theta_{H,hip}) \end{cases}, \quad (6)$$

where  $(x_k, z_k)$  denote the coordinates of the knee joint in the hip-fixed frame.  $l_T$  represents the thigh length.  $\theta_{H,hip}$  is the hip joint angle.

Foot-end coordinates  $(x_f, z_f)$  in hip-fixed frame can then be expressed as follows:

$$\begin{cases} x_f = l_T \sin(\theta_{H,hip}) + l_S \sin(\theta_{H,hip} - \theta_{H,knee}) \\ z_f = l_T \cos(\theta_{H,hip}) + l_S \cos(\theta_{H,hip} - \theta_{H,knee}) \end{cases}, \quad (7)$$

where  $l_S$  represents the shank length and  $\theta_{H,knee}$  is the knee joint angle.

Based on the force balance equation, the relationship between foot-end contact forces and joint torques can be expressed as follows:

$$\begin{cases} \hat{\tau}_{hip} = \hat{F}_{fx}z_f - \hat{F}_{fz}x_f \\ \hat{\tau}_{knee} = \hat{F}_{fx}(z_f - z_k) - \hat{F}_{fz}(x_f - x_k) \\ \hat{\tau}_{ankle} = \hat{\tau}_{fy} \end{cases}, \quad (8)$$

where  $F_{fx}, F_{fz}, \tau_{fy}$  denote the foot-end contact forces in the sagittal plane.  $\hat{\tau}_{hip}, \hat{\tau}_{knee}$  and  $\hat{\tau}_{ankle}$  denote the torques of the hip, knee, and ankle joints, respectively.

Assuming that the foot end is attached to the ground using a fixed joint for the stance phase, the relationship of the joint torques and the hip contact forces can be expressed as:

$$\begin{cases} \hat{\tau}_{hip} = \hat{\tau}_{ty} \\ \hat{\tau}_{knee} = -\hat{F}_{tx}z_k + \hat{F}_{tz}x_k \\ \hat{\tau}_{ankle} = -\hat{F}_{tx}z_f + \hat{F}_{tz}x_f \end{cases}, \quad (9)$$

Similarly, the effectiveness of the EFOC assistance method is validated by simulations. As depicted in Figure 7a, the hip, knee, and ankle joints of the human are set to position control mode, with joint angle profiles  $(Q_h(t), Q_k(t), Q_a(t))$  driving the three joints to reproduce the single-leg swing motion. The joint torques  $(\hat{\tau}_{hip}, \hat{\tau}_{knee}, \hat{\tau}_{ankle})$  are multiplied by the assistance coefficient  $\alpha$ , but instead of being applied in parallel to the corresponding joints, they are transformed to  $(\hat{F}_{fx}, \hat{F}_{fz}, \hat{\tau}_{fy})$  and applied at the foot end.

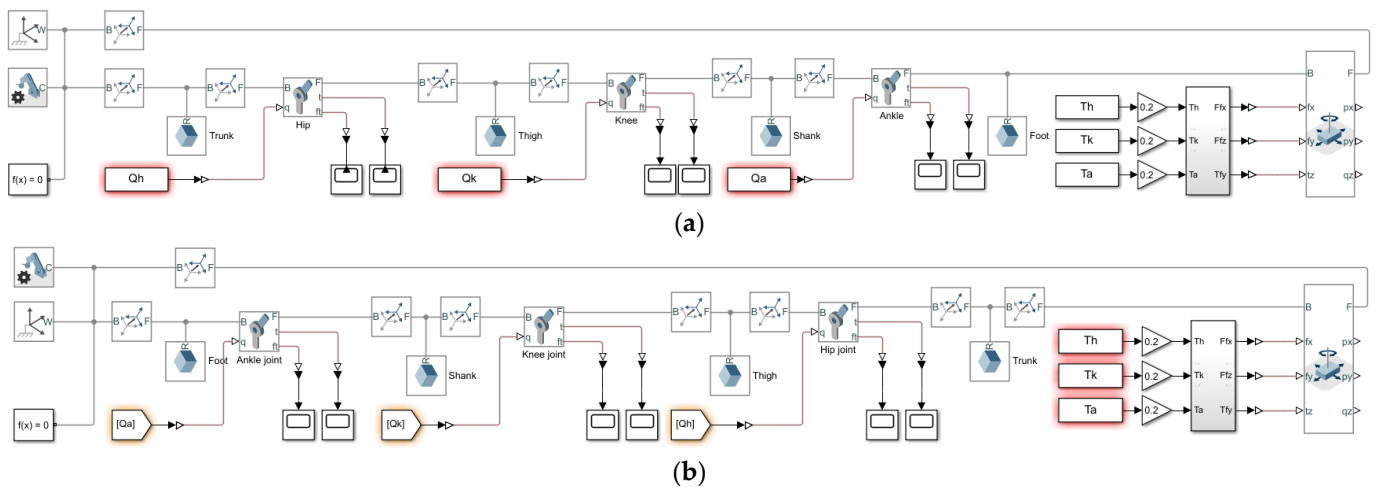


**Figure 7.** Simulation models of EFOC power assists with a single leg in the sagittal plane. (a) The simulation model of the single leg during the swing phase; (b) the simulation model of the single leg during the stance phase.



The angle profiles of the hip, knee, and ankle joints drive the stance leg in the sagittal plane during the torso squat movement. As shown in Figure 7b, the required joint torques ( $T_h(t)$ ,  $T_k(t)$ ,  $T_a(t)$ ) for squat motion multiply assistance coefficient  $\alpha$ , and the equivalent hip contact forces ( $\hat{F}_{tx}$ ,  $\hat{F}_{tz}$ ,  $\hat{t}_{ty}$ ) can be solved through Equation (9).

As illustrated in Figure 8a, the peak torques at the hip, knee, and ankle joints were reduced with the EFOC-assisted method to 43.3 Nm, 18.8 Nm, and 5.1 Nm, respectively. From Figure 8b, the joint torques of the human body after assistance were recorded and compared with the joint torques without assistance. When active assistance was applied in the form of EFOC, the peak torques at the hip, knee, and ankle joints decreased to 56.4 Nm, 226.2 Nm, and 13.6 Nm, respectively.

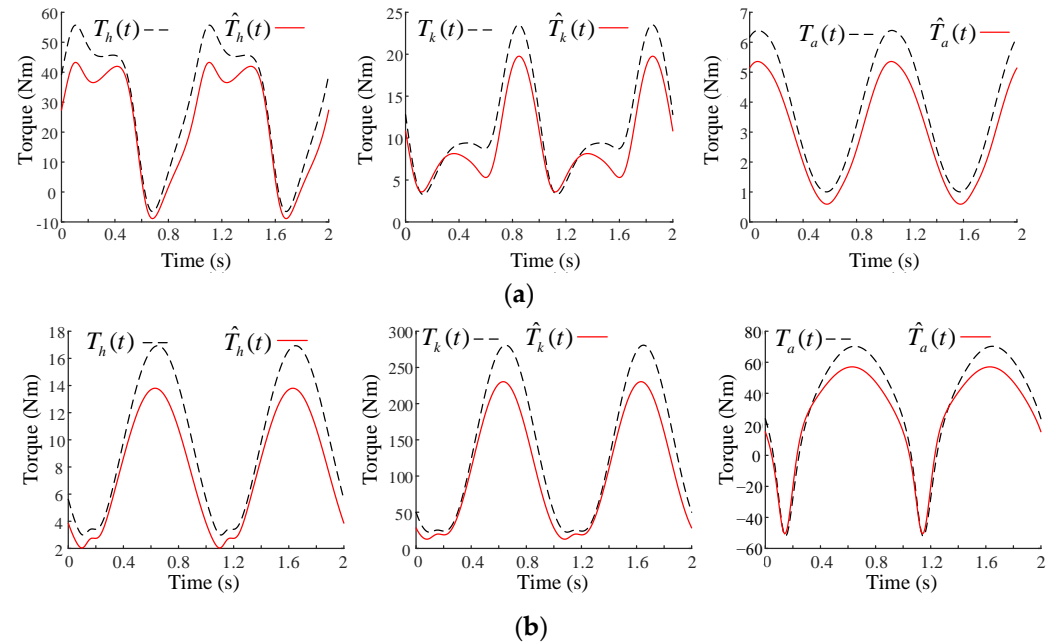


**Figure 8.** Comparison of the joint torque profiles with and without EFOC active assistance. The black dashed curves represent the joint torque profiles without assistance, while the red curves represent the joint torque profiles after assistance. (a) Joint torque profiles with and without assistance during swing motion; (b) joint torque profiles with and without assistance during squatting.

Comparing the experimental results of EFOC with those of MTPC reveals that EFOC achieves similar assistance effects to MTPC, with the following advantages:

- (1) It is not necessary for the assistance actuators of an exoskeleton robot to be parallel to each joint of the human lower limb, improving the flexibility of the configuration design.
- (2) The number of human–machine connection points is significantly reduced, allowing for the relocation of connection points to positions on the human body capable of withstanding higher loads.
- (3) It contributes to improving the loading conditions on the human skeletal system, reducing skeletal stress while decreasing muscle efforts on the human body.

#### 4. Experimental Results and Discussion

To grant the wearer absolute and active control over their movement, thereby enhancing comfort, this research departs from conventional position or velocity control methods in a hydraulic-driven lower limb exoskeleton robot [27]. Instead, we implement a force control scheme, where the exoskeleton robot is governed solely by force/torque commands, without relying on position or velocity feedback. Thereby, the exoskeleton robots only interact with the body in the form of force or torque. The force sensors are mounted on the exoskeleton robot to collect the human–exoskeleton interface forces for the force control

scheme, as shown in Figure 9. The control loop and sensor signal acquisition are both at 1 kHz.

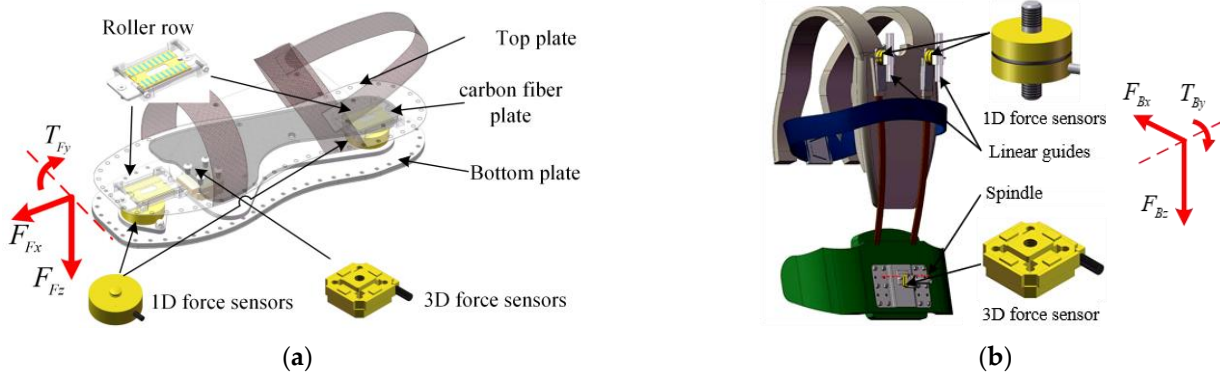


**Figure 9.** Force measurement devices are mounted on the exoskeleton robot. (a) Force sensors on shoes; (b) force sensors on backpack.

The experiment involved participants wearing the exoskeleton robot with the assistance coefficient set at 0.25. They performed squatting, stepping, and jumping motions under real-time signal acquisition from the motion capture system and the three-dimensional force platform, as shown in Figure 10. There are two active joints and four passive joints for each leg of the exoskeleton robot. The structural design, including actuators and sensors, of the exoskeleton robot is detailed in [27]. The position of the marker points on the body and the ground reaction forces were recorded, from which the joint torques of the human body were calculated. Based on the predetermined assistance coefficient and the EFOC assistance method, these torques were utilized to derive the target forces at the human-machine connection points. Simultaneously, precise force control at the human-machine connection points is achieved through human-machine interface force feedback and the feedforward dynamics of the exoskeleton robot.

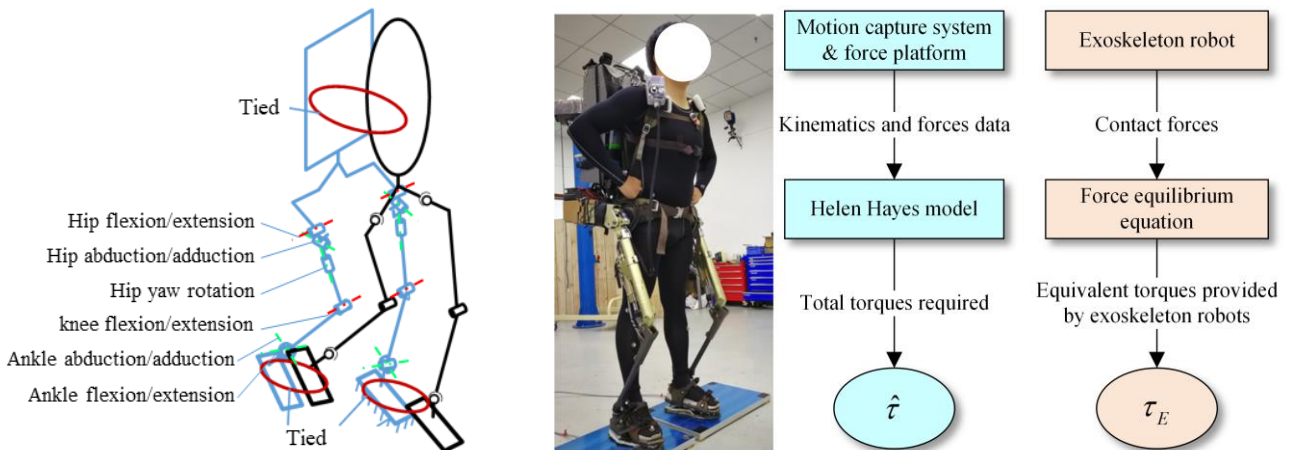


**Figure 10.** Configuration of the exoskeleton robot and the experimental test system. Red dashed lines correspond to active joints with hydraulic drive units, while blue ones correspond to passive joints.

For a comparison of the effects before and after assistance, the force sensors on the exoskeleton robot recorded the actual human-machine interface forces. The interface forces were then used to calculate the equivalent joint torques provided by the exoskeleton robot to various joints of the human body via Equations (8) and (9). The results of the experiment are shown in Figure 11.

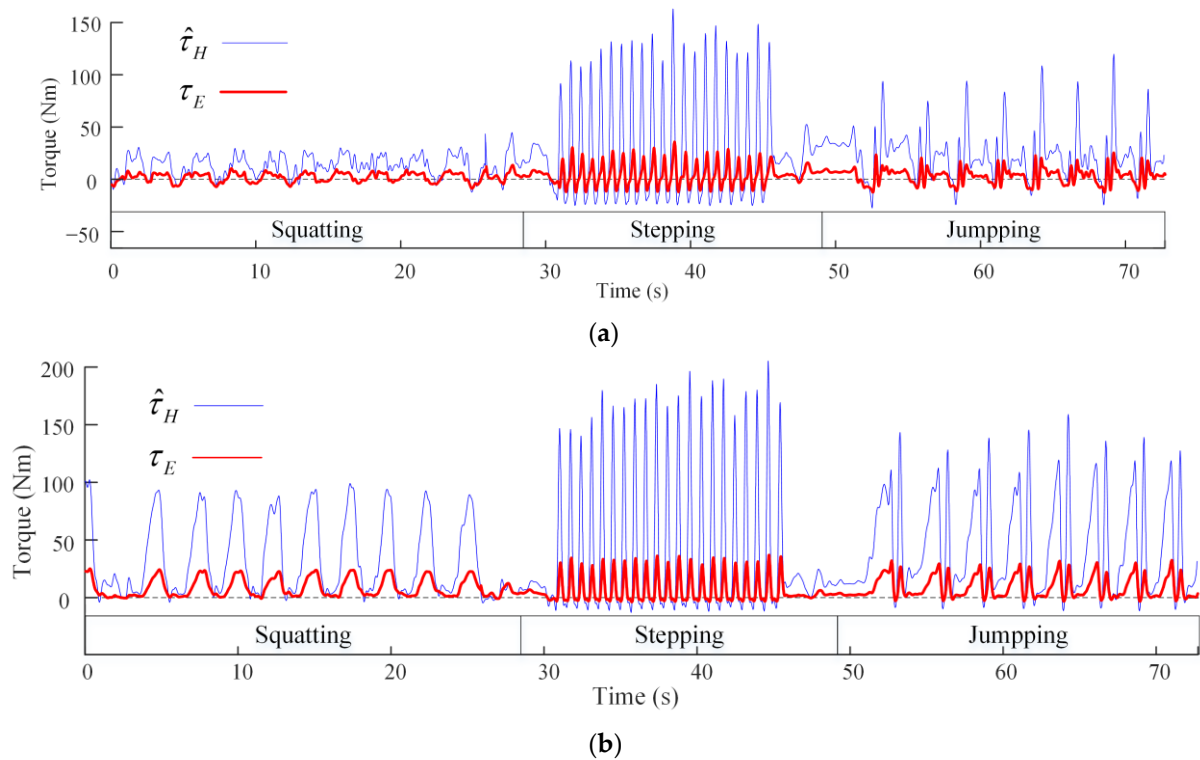


**Figure 11.** Experimental results of joint torque profiles during squatting, stepping, and jumping. (a) Hip joint torque profiles: total torques required and provided by the exoskeleton robot; (b) knee joint torque profiles: total torques required and provided by the exoskeleton robot.

The experimental results demonstrate that the wearer can naturally perform three types of movements without any specific settings, indicating good coordination between the exoskeleton and the human body. Comparing the profiles of curves  $\tau_E$  and  $\hat{\tau}_H$ , they exhibit similar shapes. As the required joint torque of the human body increases, the equivalent joint torque generated by the exoskeleton also increases accordingly, indicating that the exoskeleton robot can dynamically respond to the torque demands of the human joints. The magnitude of curve  $\tau_E$  is approximately 25% of curve  $\hat{\tau}_H$ , indicating that the exoskeleton robot accurately identifies the required joint torque of the human body across various movements and provides assistance to the human body in accordance with the preset assistance coefficient of 0.25. This experiment validates the effectiveness of the proposed EFOC assistance method.

## 5. Conclusions and Future Work

In summary, this study introduces two active assistance methods, namely the JTPC and EFOC methods. Through comparative analysis, the EFOC method demonstrates equivalent assistance effects to the JTPC method while overcoming some of its limitations. Specifically, the EFOC method facilitates the transfer of the force exerted by the exoskeleton robots on the wearer to more comfortable positions. And it reduces the demands on the structural design of the exoskeleton robots. Experimental evaluations involving squatting, stepping, and jumping locomotion were conducted using a hydraulic-driven lower limb exoskeleton robot, validating the effectiveness of the proposed EFOC assistance method.

However, there are some limitations in this work. The load-bearing capacities of various parts of the human lower limb musculoskeletal system were not thoroughly studied. For the sake of convenience in the design and wearing of the exoskeleton robot, the foot end was used as the primary load-bearing position. Additionally, this work did not consider the assistance of all six degrees of freedom of the lower limbs; instead, it was validated on an exoskeleton robot with only two active degrees of freedom.

**Author Contributions:** Conceptualization, J.D. and Y.S.; methodology, H.G., M.L. and Y.S.; software, J.D. and W.J.; validation, J.D., W.J., M.L. and Y.S.; investigation, W.J., H.G. and Y.S.; resources, J.D. and M.L.; data curation, J.D. and Y.S.; writing—original draft preparation, J.D. and Y.S.; writing—review and editing, Y.S.; supervision, W.J. and H.G.; project administration, J.D., W.J. and Y.S.; funding acquisition, W.J., M.L. and H.G. All authors have read and agreed to the published version of the manuscript.

**Funding:** This research was funded by the National Natural Science Foundation of China (No. 52305072), Natural Science Foundation of Hebei Province of China (No. E2022203095), University-Industry Collaborative Education Program (No. 220603936245709) and Shenzhen Special Fund for Future Industrial Development (No. KJZD20230923114222045).

**Data Availability Statement:** The original contributions presented in the study are included in the article, further inquiries can be directed to the corresponding author.

**Conflicts of Interest:** The authors declare no conflicts of interest.

## References

- Hussain, F.; Goecke, R.; Mohammadian, M. Exoskeleton robots for lower limb assistance: A review of materials, actuation, and manufacturing methods. *Proc. Inst. Mech. Eng. Part H J. Eng. Med.* **2021**, *235*, 1375–1385. [\[CrossRef\]](#)
- Masengo, G.; Zhang, X.; Dong, R.; Alhassan, A.B.; Hamza, K.; Mudaheranwa, E. Lower limb exoskeleton robot and its cooperative control: A review, trends, and challenges for future research. *Front. Neurobot.* **2023**, *16*, 913748. [\[CrossRef\]](#)
- Asanza, V.; Peláez, E.; Loayza, F.; Lorente-Leyva, L.L.; Peluffo-Ordóñez, D.H. Identification of lower-limb motor tasks via brain–computer interfaces: A topical overview. *Sensors* **2022**, *22*, 2028. [\[CrossRef\]](#)
- Pinto-Fernandez, D.; Torricelli, D.; del Carmen Sanchez-Villamanan, M.; Aller, F.; Mombaur, K.; Conti, R.; Vitiello, N.; Moreno, J.C.; Pons, J.L. Performance evaluation of lower limb exoskeletons: A systematic review. *IEEE Trans. Neural Syst. Rehabil. Eng.* **2020**, *28*, 1573–1583. [\[CrossRef\]](#)
- Puyuelo-Quintana, G.; Cano-De-La-Cuerda, R.; Plaza-Flores, A.; Garcés-Castellote, E.; Sanz-Merodio, D.; Goñi-Arana, A.; Marín-Ojea, J.; García-Armada, E. A new lower limb portable exoskeleton for gait assistance in neurological patients: A proof of concept study. *J. NeuroEng. Rehabil.* **2020**, *17*, 1–16. [\[CrossRef\]](#)
- Gholap, R.; Thorat, S.; Chavan, A. Review of current developments in lower extremity exoskeleton systems. *Mater. Today Proc.* **2023**, *72*, 817–823. [\[CrossRef\]](#)
- Jezernik, S.; Colombo, G.; Keller, T.; Frueh, H.; Morari, M. Robotic orthosis lokomat: A rehabilitation and research tool. *Neuromodul. Technol. Neural Interface* **2003**, *6*, 108–115. [\[CrossRef\]](#)
- Esquenazi, A.; Talaty, M.; Packel, A.; Saulino, M. The ReWalk powered exoskeleton to restore ambulatory function to individuals with thoracic-level motor-complete spinal cord injury. *Am. J. Phys. Med. Rehabil.* **2012**, *91*, 911–921. [\[CrossRef\]](#)
- Gad, P.; Gerasimenko, Y.; Zdunowski, S.; Turner, A.; Sayenko, D.; Lu, D.C.; Edgerton, V.R. Weight bearing over-ground stepping in an exoskeleton with non-invasive spinal cord neuromodulation after motor complete paraplegia. *Front. Neurosci.* **2017**, *11*, 333. [\[CrossRef\]](#)
- Paulo, J.; Peixoto, P.; Nunes, U.J. ISR-AIWALKER: Robotic walker for intuitive and safe mobility assistance and gait analysis. *IEEE Trans. Hum.–Mach. Syst.* **2017**, *47*, 1110–1122. [\[CrossRef\]](#)
- Baniqued, P.D.E. A Brain-Computer Interface Integrated with Virtual Reality and Robotic Exoskeletons for Enhanced Visual and Kinaesthetic Stimuli. Ph.D. Thesis, University of Leeds, Leeds, UK, 2022.
- Triloka, J.; Senanayake, S.A.; Lai, D. Neural computing for walking gait pattern identification based on multi-sensor data fusion of lower limb muscles. *Neural Comput. Appl.* **2017**, *28*, 65–77. [\[CrossRef\]](#)
- Lim, D.H.; Kim, W.S.; Kim, H.J.; Han, C.S. Development of real-time gait phase detection system for a lower extremity exoskeleton robot. *Int. J. Precis. Eng. Manuf.* **2017**, *18*, 681–687. [\[CrossRef\]](#)
- Huang, R.; Cheng, H.; Chen, Y.; Chen, Q.; Lin, X.; Qiu, J. Optimisation of reference gait trajectory of a lower limb exoskeleton. *Int. J. Soc. Robot.* **2016**, *8*, 223–235. [\[CrossRef\]](#)
- Deng, M.; Li, Z.; Kang, Y.; Chen, C.P.; Chu, X. A learning-based hierarchical control scheme for an exoskeleton robot in human–robot cooperative manipulation. *IEEE Trans. Cybern.* **2018**, *50*, 112–125. [\[CrossRef\]](#)
- Li, N.; Yan, L.; Qian, H.; Wu, H.; Wu, J.; Men, S. Review on lower extremity exoskeleton robot. *Open Autom. Control Syst. J.* **2015**, *7*, 441–453.
- Heo, G.S.; Lee, S.R.; Kwak, M.K.; Park, C.W.; Kim, G.; Lee, C.Y. Motion control of bicycle-riding exoskeleton robot with interactive force analysis. *Int. J. Precis. Eng. Manuf.* **2015**, *16*, 1631–1637. [\[CrossRef\]](#)
- Zeng, Y.; Yang, J.; Yin, Y. Gaussian process-integrated state space model for continuous joint angle prediction from EMG and interactive force in a human-exoskeleton system. *Appl. Sci.* **2019**, *9*, 1711. [\[CrossRef\]](#)
- Kazerooni, H.; Racine, J.L.; Huang, L.; Steger, R. On the control of the berkeley lower extremity exoskeleton (BLEEX). In Proceedings of the 2005 IEEE International Conference on Robotics and Automation (ICRA), Barcelona, Spain, 18–22 April 2005; pp. 4353–4360.

20. Li, K.; Zhang, J.; Wang, L.; Zhang, M.; Li, J.; Bao, S. A review of the key technologies for sEMG-based human-robot interaction systems. *Biomed. Signal Process. Control* **2020**, *62*, 102074. [[CrossRef](#)]
21. Benabid, A.L.; Costecalde, T.; Eliseyev, A.; Charvet, G.; Verney, A.; Karakas, S.; Foerster, M.; Lambert, A.; Morinière, B.; Abroug, N.; et al. An exoskeleton controlled by an epidural wireless brain-machine interface in a tetraplegic patient: A proof-of-concept demonstration. *Lancet Neurol.* **2019**, *18*, 1112–1122. [[CrossRef](#)]
22. Wang, Z. *Iterative Learning Control for Lower Limb Exoskeleton Robot*; The University of Manchester: Manchester, UK, 2022.
23. Tiboni, M.; Borboni, A.; Vèrité, F.; Bregoli, C.; Amici, C. Sensors and Actuation Technologies in Exoskeletons: A Review. *Sensors* **2022**, *22*, 884. [[CrossRef](#)]
24. Borboni, A.; Villafañe, J.H.; Mullè, C.; Valdes, K.; Faglia, R.; Taveggia, G.; Negrini, S. Robot-Assisted Rehabilitation of Hand Paralysis After Stroke Reduces Wrist Edema and Pain: A Prospective Clinical Trial. *J. Manip. Physiol. Ther.* **2017**, *40*, 21–30. [[CrossRef](#)]
25. Li, M.; Deng, J.; Zha, F.; Qiu, S.; Wang, X.; Chen, F. Towards online estimation of human joint muscular torque with a lower limb exoskeleton robot. *Appl. Sci.* **2018**, *8*, 1610. [[CrossRef](#)]
26. *MATLAB, Version R2021b*; The MathWorks, Inc.: Natick, MA, USA, 2021. Available online: <https://www.mathworks.com/products/matlab.html> (accessed on 1 January 2023).
27. Deng, J.; Wang, P.; Li, M.; Guo, W.; Zha, F.; Wang, X. Structure design of active power-assist lower limb exoskeleton APAL robot. *Adv. Mech. Eng.* **2017**, *9*, 1687814017735791. [[CrossRef](#)]

**Disclaimer/Publisher’s Note:** The statements, opinions and data contained in all publications are solely those of the individual author(s) and contributor(s) and not of MDPI and/or the editor(s). MDPI and/or the editor(s) disclaim responsibility for any injury to people or property resulting from any ideas, methods, instructions or products referred to in the content.